Pressure-Induced Transition in Magnetoresistance of Single-Walled Carbon Nanotubes

J. Z. Cai,[1] L. Lu,[1,2,*] W. J. Kong,[1] H. W. Zhu,[3] C. Zhang,[4] B. Q. Wei,[3] D. H. Wu,[5] and Feng Liu[2,6]

[1]*Institute of Physics, Chinese Academy of Sciences, Beijing 10080, China*

[2]*International Center for Quantum Structures, Chinese Academy of Sciences, Beijing 10080, China*

[3]*Department of Electrical and Computer Engineering, Louisiana State University, Baton Rouge, Louisiana 70803, USA*

[4]*School of Engineering Physics, University of Wollongong, Wollongong 2522, Australia*

[5]*Department of Mechanical Engineering, Tsinghua University, Beijing 10084, China*

[6]*Department of Materials Science and Engineering, University of Utah, Salt Lake City, Utah 84112, USA*

(Received 2 September 2005; published 11 July 2006)

We applied hydrostatic pressure (up to 10 GPa) to single-walled carbon nanotube bundles at low temperature (down to 2 K) to measure their magnetoresistance (MR) in a field up to 12 T. We found a pressure-induced transition in MR from positive to negative in the high-field regime. The onset of the transition occurs at ~1.5 GPa, which correlates closely with the tube shape transitions. The characteristics of the high-pressure MR are consistent with a model of pressure-induced two-dimensional weak localization.

DOI: 10.1103/PhysRevLett.97.026402 PACS numbers: 71.30.+h, 73.63.Fg

The electronic and transport properties of single-walled carbon nanotubes (SWNTs) have attracted considerable interest [1,2] because of their potential application in electronic devices. One outstanding feature of SWNTs is the strong correlation between their electronic and structural properties: they can be either metallic or semiconducting depending on their diameter and chirality [3]. Furthermore, their electric properties display a high sensitivity to structural deformation [4,5], providing a useful mechanism for designing electromechanical sensors and devices.

One way to deform SWNTs is by applying hydrostatic pressure [6,7]. Experiments [8–10] have shown structural phase transitions of SWNT bundles under hydrostatic pressure. First-principles calculations predicted that in addition to structural transition, pressure can induce electric transition, e.g., making a metallic armchair SWNT semiconducting [4,5]. The electron transport properties of SWNT bundles were studied below 2 GPa by using a piston-type pressure cell [11] and above 3 GPa by a sintered diamond anvil cell (DAC) [12]. In the former case an anomaly was observed at ~1.4 GPa. Here, we present experimental measurements of magnetoresistance (MR) of SWNT bundles under hydrostatic pressure. Our study will help to reveal the transport mechanisms of SWNTs in a magnetic field under pressure, and to shed light on the potential application of SWNT pressoelectronic and magnetoelectronic devices.

Our measurements are carried out under some extreme conditions, with a hydrostatic pressure up to 10 GPa, a low temperature down to 2 K, and a high magnetic field up to 12 T. The superlong SWNT bundles were synthesized by a ferrocene-assisted chemical vapor deposition technique [13] at 1050–1300 K. The energy dispersive x-ray microanalysis shows the raftlike SWNT bundles contain impurities (~5% wt) of Fe particles and amorphous carbon. Both metallic and semiconducting SWNTs coexist, whereas a sharp Raman peak at 215.6 cm^{-1} suggests that the metallic (11,5) tubes are the dominant species [13,14].

SWNT bundles of $\sim 0.6 \times 0.01 \times 0.003$ mm^3 in volume were used for the measurements. The whole pressure range from 0 to 11.4 GPa was covered by using two types of pressure cells. The three sets of data at low pressures of 0, 0.5, and 1.0 GPa were taken by using a piston-type pressure cell, with the sample immersed in a liquid pressure medium (diffusion pump oil mixed with ethanol at a ratio of 1:1). The data at 1.5 GPa and above were taken by using a sintered DAC with a mixture of steatite powder and five minutes epoxy as the pressure medium [15–17]. Both pressure cells are made of Cu-Be alloy for matching the quantum-design physical property measurement system Dewar. The pressure of the DAC is calibrated by using the superconducting transition temperature of Pb, with an accuracy of ± 0.3 GPa.

To measure the transport properties under pressure, four gold wires of 25 μm diameter were arranged regularly on the sample in the pressure cell, as illustrated in Fig. 1, inset 1. A scanning dc current plus a small ac current of 0.1 μA and 30.90 Hz, generated by a master-slaver-type dc + ac current source and monitored by a lock-in amplifier and a dc voltmeter, were applied to the SWNT bundles through two outside electrodes. The resulting voltage between the two inner electrodes was measured using another lock-in amplifier and dc voltmeter. Figure 1 shows the measured resistance as a function of temperature at zero pressure (i.e., vacuum) without magnetic field, and inset 2 shows the differential conductance versus the bias voltage drop between the inner electrodes. The results are consistent with the early studies under similar conditions [1].

Hydrostatic pressure was gradually increased from zero pressure to 10 GPa. At each pressure we cooled down the sample to low temperatures and measured their MR, defined as $\frac{R(B,T,P)-R(0,T,P)}{R(0,T,P)}$, by scanning the magnetic field

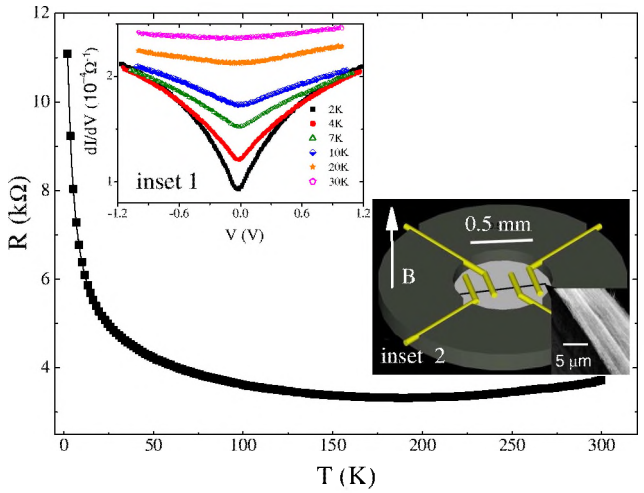

FIG. 1 (color online). The SWNT bundles' resistance vs temperature at zero pressure and in zero magnetic field. Inset 1: schematic illustration of the four-probe measurement in the DAC, together with a scanning electron microscope image of the sample. The magnetic field is perpendicular to the tubes axes. Inset 2: measured differential conductance vs bias voltage.

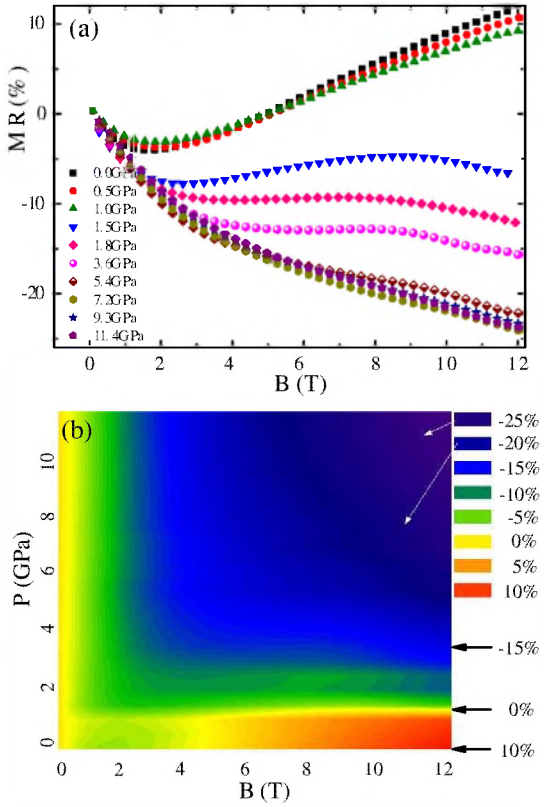

FIG. 2 (color online). (a) The field dependence of MR at different pressures. The curves from 1.5 to 3.5 GPa show the transition region. (b) Contour plot of MR as the functions of pressure and magnetic field.

from 0 to 12 T. In Fig. 2(a) the MR at 2 K is plotted versus field B under different pressures. The data can be classified into three groups. From 0 to 1.0 GPa the MR curves roughly collapse with each other, showing a nonmonotonic dependence on B and changing from negative to positive at ~2 T. This agrees well with the previous measurements [18,19] at ambient pressure. The negative-to-positive MR transition with increasing field was suggested to be induced by the field modified electron density of states (DOS) or by a metal-semiconductor transition [19]. Under high pressures (5.5–11.4 GPa) the MR curves roughly collapse with each other onto another trend, decreasing monotonically with increasing field. And under intermediate pressures (1.5–3.5 GPa), the MR displays a very weak dependence and small variation with the field.

The apparent difference between the high- and low-pressure MR data is further shown in a contour plot in Fig. 2(b): a red region below ~1.5 GPa of positive MR and a blue region above ~3.5 GPa of negative MR in high fields. This indicates a pressure-induced MR transition, with a transition pressure coinciding with the known pressure for tube shape transitions [5,8–10].

Next, we discuss the possible physical mechanisms underlying the pressure-induced MR transition. Under low pressures, all the SWNTs retain a circular shape so that their intrinsic electronic structure and intertube coupling strength remain essentially intact. And the electron transport in each SWNT is mainly ballistic. The intertube coupling and occasional tube-tube crossing within the bundles provide some small probability for the electrons hopping between different tubes, which gives rise to electron weak localization and a negative MR with a relatively long phase coherence length (hence the MR is limited only in low fields). The positive MR in high fields is probably due to a DOS effect as mentioned above.

Under sufficiently high pressure above a critical value [5,6], SWNTs will undergo a shape transition changing their cross section from circular to elliptical then to peanut shape. Such a transition, happening collectively to all tubes in the bundle, may enhance the intertube e-e scattering and hopping in the flattened plane, and hence induce the two-dimensional weak localization (2DWL) leading to a negative MR in high magnetic fields. Detailed analysis shows that our measured field, temperature, and pressure dependence of MR are all consistent with the 2DWL model in high fields.

In the 2DWL model, the magnetoconductance (MC) is given as [20]

$$\Delta G(B,T) = G(B,T) - G(0,T) = \Gamma\left[\psi\left(\frac{1}{2}+\frac{1}{x}\right) + \ln(x)\right], \quad (1)$$

where ψ is the digamma function, $x = B/B_\phi$, and B_ϕ is the 2DWL theory scaling parameter defined as $B_\phi = \frac{\hbar}{4eD\tau_\phi} = \frac{\hbar}{4eL_\phi^2}$, where τ_ϕ is the phase coherence time and L_ϕ is the

phase coherence length related to the inelastic and spin-spin scattering processes. We have added a prefactor Γ as a fitting parameter, to describe the possible pressure-induced DOS and sample geometry changes. The scaling parameter B_ϕ depends on temperature. For a system of 2DWL, it should follow the scaling law that the MC at different temperatures collapse onto a universal curve, as described by Eqn. (1) after scaling the field by B_ϕ i.e., $\Delta G(B,T) = F(B/B_\phi)$. Indeed, our measured field dependence of MC data obey convincingly the scaling law, as shown in Fig. 3. Furthermore, according to the 2DWL theory, B_ϕ should have a power-law relation with temperature, i.e., $B_\phi \propto T^p$, with p depending on the dominant mechanism of dephasing scattering. This is again shown for all the data above the transition pressure. Using the data at 4.2 GPa as an example, we plot B_ϕ versus T (lower inset of Fig. 3). A linear dependence is found with $p = 1$, indicating the e-e scattering is likely the dominant dephasing mechanism [21].

The degree of 2DWL is controlled by the amount of magnetic flux (compared to h/e) in a characteristic area of L_ϕ^2. One can look at two length scales to make the comparison: the magnetic length $L_B = \sqrt{\frac{\hbar}{eB}}$ and the phase coherence length $L_\phi = \sqrt{\frac{\hbar}{4eB_\phi}}$. Changing either L_B or L_ϕ shall change the degree of 2DWL and hence the MR. In general, the magnetic field suppresses the localization. For a system of fixed L_ϕ, i.e., for the present case of fixed pressure, increasing the field will decrease L_B, leading to a negative MR. This is consistent with the observed negative MR at high pressures (above the transition pressures) in the high-field regime.

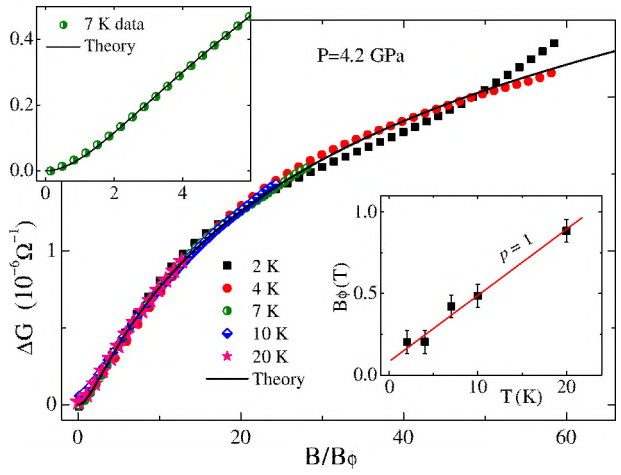

FIG. 3 (color online). ΔG at different temperatures as a function of scaled field (B/B_ϕ) collapse onto a universal curve (the solid line), as described by Eq. (1) predicted by the 2DWL theory. Upper left inset: detailed comparison in low fields between the data measured at 7 K and theory. Lower right inset: the fitting parameter B_ϕ vs temperature, showing a linear dependence corresponding to $p = 1$.

Conversely, for a system of fixed L_B, i.e., fixed magnetic field, increasing the pressure will increase the tube shape distortion, which in turn increases the degree of disorder and localization by decreasing L_ϕ, and hence increases the MR. We have derived an empirical relation between the L_ϕ and pressure (P) by discovering a scaling law of B_ϕ with respect to P at a given temperature. Taking the data at 2.2 K as an example, we plot the high-pressure data (above the transition) as a function of field scaled by B_ϕ, as shown in Fig. 4(a). Clearly, all the data at different pressures collapse onto a single curve after scaling as predicted by Eq. (1), suggesting they obey a scaling law similar to that with respect to temperature as shown in Fig. 3. Further, B_ϕ is found to be inversely proportional to P, as shown in the lower inset of Fig. 4(a). This relation is only followed by the high-pressure data (>3.5 GPa), i.e., the data above the transition pressure. While those data below the transition pressure, such as the data of 1.6 GPa, do not belong to the

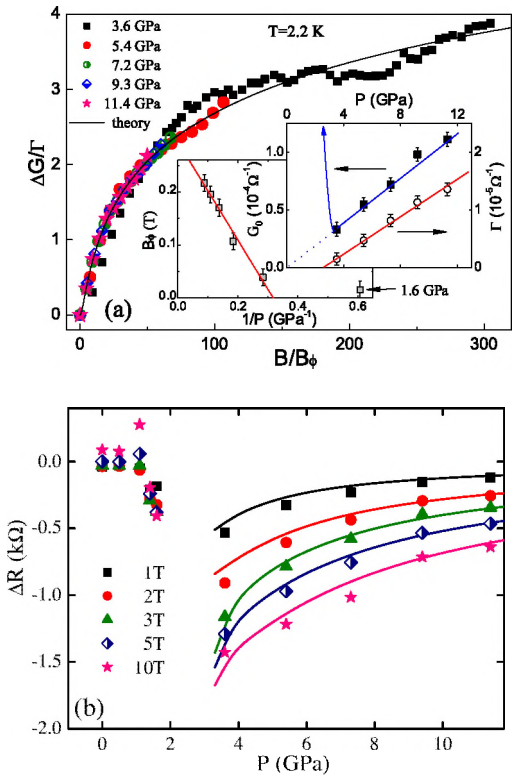

FIG. 4 (color online). (a) Scaled $\Delta G/\Gamma$ at different pressures as a function of scaled field B/B_ϕ, collapsing onto a universal curve as described by Eq. (1) (the solid line), illustrating a similar scaling law as to temperature. Lower inset: The fitting parameter B_ϕ vs $1/P$, showing an inverse linear dependence of B_ϕ on P. Upper inset: The fitting parameter Γ vs P (circles). Also plotted is the zero-field conductance $G_0 = G(0, 2.2\ \mathrm{K}, P)$ (squares). Both show a linear pressure dependence. (b) ΔR at different fields vs pressure. The solid lines are from 2DWL theory using the empirical relation between B_ϕ and P as derived in the inset of (a).

same class. This shows that only under high pressure, the data follows the 2DWL behavior.

In the upper inset of Fig. 4(a), we plotted the pressure dependencies of the zero-field conductance $G_0 \equiv G(0, 2.2\ \mathrm{K}, P)$ and of the MC amplitude Γ (the fitting parameter). The G_0 at zero pressure is very high (out of scale), as indicated by the arrow in the figure. It drops sharply at the transition pressure, demonstrating a pressure-induced metal-to-semiconductor transition as predicted by theory [5]. Above the transition pressure, both G_0 and Γ increase linearly with increasing pressure. Extrapolating the G_0 curve to zero pressure would result in a zero conductance, i.e., an insulating state if no transition existed. The linear P dependence of G_0 reflects the effect of the pressure enhanced electron wave function overlap or DOS increase, whereas the linear P dependence of Γ reflects the onset and gradual increase of MC above the critical pressure.

Specifically, we have derived an empirical relation between B_ϕ and P by a simple fitting to the data, which gives rise to $B_\phi = A(\frac{1}{P_0} - \frac{1}{P})$ with $P_0 = 3.1$ GPa. Then, it is straightforward to see that $L_\phi \propto \sqrt{\frac{1}{B_\phi}} \propto \sqrt{\frac{P_0 P}{P - P_0}}$. Thus, the effect of pressure, which increases the tube shape distortion and hence the e-e scattering between the tubes, can be effectively characterized by its effect on L_ϕ. At a given field, the higher the pressure, the shorter the L_ϕ, and then the smaller the MR. In Fig. 4(b), we plot $\Delta R = R(B, T, P) - R(0, T, P)$ as a function of P for different magnetic fields, and fitted the data using Eq. (1) of the 2DWL model and the derived empirical relation between L_ϕ and P. The results once again show that the agreement between the theory (solid lines) and the experiment is fairly good at all pressures above the transition pressure.

The above analysis shows that the field, temperature, and pressure dependence of the measured MC data are all consistent with the 2DWL theory. In particular, the field-dependence data in low fields agree with the theory (upper inset of Fig. 3), obeying the expected parabolic law when B/B_ϕ is small. The scaling law seemed to even sustain to relatively higher fields, but the agreement is less good. However, we cannot rule out completely other possible mechanisms. For example, a pressure-induced metal-insulator transition similar to the doping effect, might cause a MR transition in high fields as shown by Vavro *et al.* [19]. We also tried to fit the data with a 3DWL model, but the agreement is much worse.

We have repeated the experiments on three samples, which all show consistently the same behavior. The MR curves were measured at given pressures and temperatures by changing the magnetic field in multiple cycles, and the data are completely reversible. However, we could not show the reversibility with respect to pressure, because pressure can only be increased in our experimental setup. Upon decreasing pressure, the gasket sealing will collapse and the electrodes will break off from the sample. On the other hand, recent x-ray diffraction experiments [22] have indicated the structure and lattice symmetry of SWNT bundles can be reversible under pressure up to 13 GPa.

In conclusion, we have measured the MR of the SWNT bundles under extreme conditions of high magnetic field, low temperature, and high pressure. We observe a pressure-induced positive-to-negative MR transition in the high-field regime. The onset of the transition correlates closely with the pressure-induced shape transitions in SWNTs. Our measurements indicate that the MR transition is consistent with the 2DWL model. The data further suggest that the 2DWL is possibly dominated by the e-e scattering in between the tubes, which depends on the magnetic field and pressure through tube shape distortions.

We thank M. Nunez-Regueiro for introducing us to the DAC technique and the zero-field data of SWNTs prior to publication. This work is supported by the Knowledge Innovation Program of CAS and the NSFC. F. Liu thanks for support from DOE.

*Electronic address: lilu@aphy.iphy.ac.cn

[1] M. Bockrath *et al.*, Nature (London) **397**, 598 (1999).
[2] A. Bachtold *et al.*, Nature (London) **397**, 673 (1999).
[3] Jeroen W. G. Wildoer *et al.*, Nature (London) **391**, 59 (1998).
[4] Jun-Qiang Lu *et al.*, Phys. Rev. Lett. **90**, 156601 (2003).
[5] Jian Wu *et al.*, Phys. Rev. B **69**, 153406 (2004).
[6] Ji Zang *et al.*, Phys. Rev. Lett. **92**, 105501 (2004).
[7] D. Y. Sun *et al.*, Phys. Rev. B **70**, 165417 (2004).
[8] Jie Tang *et al.*, Phys. Rev. Lett. **85**, 1887 (2000).
[9] U. D. Venkateswaran *et al.*, Phys. Rev. B **59**, 10 928 (1999).
[10] M. J. Peters *et al.*, Phys. Rev. B **61**, 5939 (2000).
[11] Jie Tang *et al.*, J. Phys. Condens. Matter **14**, 10 575 (2002).
[12] M. Monteverde and M. Nunez-Regueiro, Phys. Rev. Lett. **94**, 235501 (2005).
[13] H. W. Zhu *et al.*, Science **296**, 884 (2002).
[14] Bingqing Wei *et al.*, Nano Lett. **2**, 1105 (2002).
[15] K. J. Dunn and F. P. Bundy, Rev. Sci. Instrum. **49**, 365 (1978).
[16] F. P. Bundy, Rev. Sci. Instrum. **46**, 1318 (1975).
[17] S. Sanfilippo *et al.*, Phys. Rev. B **61**, R3800 (2000).
[18] G. T. Kim *et al.*, Phys. Rev. B **58**, 16 064 (1998).
[19] J. Vavro, J. M. Kikkawa, and J. E. Fischer, Phys. Rev. B **71**, 155410 (2005).
[20] Patrick A. Lee *et al.*, Rev. Mod. Phys. **57**, 287 (1985).
[21] B. L. Altshuler *et al.*, J. Phys. C **15**, 7367 (1982).
[22] S. M. Sharma *et al.*, Phys. Rev. B **63**, 205417 (2001).